Multipath Mitigation in Global Navigation Satellite Systems Using a Bayesian Hierarchical Model with Bernoulli Laplacian Priors - Supplementary Material.

Julien LESOUPLE[1], Jean-Yves TOURNERET[1,2], Mohamed SAHMOUDI[1,3], Franck BARBIERO[4] and Frédéric FAURIE[5]

[1]TéSA, 7 Boulevard de la Gare, 31500 Toulouse, France
[2]ENSEEIHT-IRIT, 2 Rue Camichel, 31071 Toulouse, France
[3]ISAE Supaero, 10 Avenue Edouard Belin, 31400, Toulouse, France
[4]CNES, 18 Avenue Edouard Belin, 31400, Toulouse, France
[5]M3 Systems, 26 Rue du Soleil Levant, 31410, Lavernose, France

October 24, 2018

Abstract

This document contains supplementary materials associated with the conference paper [1].

1 Introduction

The aim of the paper [1] was to introduce a Bayesian estimation method for the multipath (MP) biases and the associated hyperparameters in Global Navigation Satellite Systems (GNSS) measurements (pseudoranges and Doppler). To do so, we supposed the receiver has s_k satellites in view, and thus has access to $2s_k$ measurements (s_k pseudoranges and s_k pseudorange rates) which can be expressed as

$$\boldsymbol{y}_k = \bar{\boldsymbol{H}}_k \boldsymbol{x}_k + \boldsymbol{m}_k + \boldsymbol{n}_k \tag{1}$$

where $\boldsymbol{y}_k = (y_{i,k})_{i=1,\dots,2s_k} \in \mathbb{R}^{2s_k}$ is a vector containing the differences between the measurements and their estimates, $\bar{\boldsymbol{H}}_k \in \mathbb{R}^{2s_k \times 8}$ is a block diagonal matrix with two blocks equal to the Jacobian matrix of the problem denoted as $\boldsymbol{H}_k$, and $\boldsymbol{n}_k$ is an additive white Gaussian noise with covariance matrix $\boldsymbol{R}_k$. In order to account for different noise variances for the pseudoranges and pseudorange rates, we assume in [1] that $\boldsymbol{R}_k = \mathrm{diag}(\sigma_{i,k}^2) \in \mathbb{R}^{2s_k \times 2s_k}$ is a diagonal matrix, with

$$\sigma_{i,k}^2 = \begin{cases} c_{1,k}\mu_{i,k}, \ i = 1, \dots, s_k, \\ c_{2,k}\mu_{i,k}, \ i = s_k + 1, \dots, 2s_k \end{cases}$$

where

$$\mu_{i,k} = 10^{-\frac{(C/N_0)_{i,k}}{10}}$$

is related to the signal to noise ratio in the ith channel at time instant k (provided by standard receivers). Note that this formulation was proposed in [2] with $c_{1,k} = 1.1 \times 10^4$ m^2. In this paper, we will use $c_{2,k} = 1.1 \times 10^2$ m^2.s^{-2}, in order to have a pseudorange variance 100 times larger than the pseudorange rate variance.

2 Hierarchical model

We recall here the model investigated in [1]. Using the notation $\bar{\boldsymbol{h}}_{i,k}$ for the ith line of matrix $\bar{\boldsymbol{H}}_k$ for $i = 1, \ldots, 2s_k$, this model is defined as follows

$$
\begin{aligned}
y_{i,k}|\boldsymbol{x}_k, m_{i,k}, \sigma^2_{i,k} &\sim \mathcal{N}(\bar{\boldsymbol{h}}_{i,k}\boldsymbol{x}_{1,k} + m_{i,k}, \sigma^2_{i,k}), \quad i = 1, ..., s_k & (2)\\
&\sim \mathcal{N}(\bar{\boldsymbol{h}}_{i,k}\boldsymbol{x}_{2,k} + m_{i,k}, \sigma^2_{i,k}), \quad i = s_k+1, ..., 2s_k & (3)\\
m_{i,k}|z_{i,k}, \tau^2_{i,k} &\sim \begin{cases} \delta(m_{i,k}) & \text{if } z_{i,k} = 0 \\ \mathcal{N}(m_{i,k}|0, c_{1,k}\tau^2_{i,k}) & \text{if } z_{i,k} = 1 \end{cases}, \quad i = 1, ..., s_k & (4)\\
&\sim \begin{cases} \delta(m_{i,k}) & \text{if } z_{i,k} = 0 \\ \mathcal{N}(m_{i,k}|0, c_{2,k}\tau^2_{i,k}) & \text{if } z_{i,k} = 1 \end{cases}, \quad i = s_k+1, ..., 2s_k & (5)\\
\tau^2_{i,k}|a_{1,k}, a_{2,k} &\sim \mathcal{E}\left(\tau^2_{i,k} \middle| \frac{2}{w^2_{i,k}a^2_{1,k}}\right), \quad i = 1, ..., s_k & (6)\\
&\sim \mathcal{E}\left(\tau^2_{i,k} \middle| \frac{2}{w^2_{i,k}a^2_{2,k}}\right), \quad i = s_k+1, ..., 2s_k & (7)\\
z_{i,k}|p_{1,k}, p_{2,k} &\sim \mathcal{B}(z_{i,k}|p_{1,k}), \quad i = 1, ..., s_k & (8)\\
&\sim \mathcal{B}(z_{i,k}|p_{2,k}), \quad i = s_k+1, ..., 2s_k & (9)\\
f(a^2_{j,k}) &\propto 1/a^2_{j,k}, \quad j = 1, 2 & (10)\\
p_{j,k} &\sim \mathcal{U}_{[0,1]}(p_{j,k}), \quad j = 1, 2 & (11)\\
\boldsymbol{x}_k = (\boldsymbol{x}^T_{1,k}, \boldsymbol{x}^T_{2,k})^T &\sim \mathcal{N}(\boldsymbol{0}_8, \boldsymbol{F}_k\boldsymbol{P}_{k|k}\boldsymbol{F}^T_k + \boldsymbol{Q}_k). & (12)
\end{aligned}
$$

The conditional distributions of each parameter can be computed as detailed in the next section. Note that these distributions are also conditioned upon $\boldsymbol{y}_{1:k-1}$. However, for brevity, we have not indicated this condition, which only appears in the matrix $\boldsymbol{P}_{k|k}$ and in the linearization point $\{\tilde{\boldsymbol{r}}^T_k, \tilde{\boldsymbol{v}}^T_k\}^T$.

3 Conditional distributions

3.1 Conditional distribution of $\tau^2_{i,k}$

We have, for $i = 1, ..., s_k$ for instance

$$
\begin{aligned}
f(\tau^2_{i,k}|m_{i,k}, a_1, z_{i,k}) &\propto f(m_{i,k}|z_{i,k}, \tau^2_{i,k})f(\tau^2_{i,k}|a_{1,k})\\
&\propto \begin{cases} \exp\left(-\frac{w^2_{i,k}a^2_j\tau^2_{i,k}}{2}\right) & \text{if } z_{i,k} = 0 \\ \exp\left(-\frac{w^2_{i,k}a^2_1\tau^2_{i,k}}{2}\right)(\tau^2_{i,k})^{-1/2}\exp\left(-\frac{m^2_{i,k}}{2c_{1,k}\tau^2_{i,k}}\right) & \text{if } z_{i,k} = 1 \end{cases}\\
&\propto \begin{cases} \exp\left(-\frac{w^2_{i,k}a^2_1\tau^2_{i,k}}{2}\right) & \text{si } z_{i,k} = 0 \\ (\tau^2_{i,k})^{-1/2}\exp\left(-\frac{1}{2}\left(w^2_{i,k}a^2_1\tau^2_{i,k} + \frac{m^2_{i,k}/c_{1,k}}{\tau^2_{i,k}}\right)\right) & \text{si } z_{i,k} = 1 \end{cases}
\end{aligned}
\tag{13}
$$

hence

$$
f(\tau^2_{i,k}|m_{i,k}, a^2_{1,k}, z_{i,k}) = \begin{cases} \mathcal{E}\left(\tau^2_{i,k} \middle| \frac{2}{w^2_{i,k}a^2_1}\right) & \text{if } z_{i,k} = 0 \\ \mathcal{GIG}\left(\tau^2_{i,k} \middle| \frac{1}{2}, w^2_{i,k}a^2_1, \frac{m^2_{i,k}}{c_{1,k}}\right) & \text{if } z_{i,k} = 1 \end{cases}, \quad i = 1, ..., s_k \tag{14}
$$

where $\mathcal{GIG}(.|p, a, b)$ is the Generalized Inverse Gaussian distribution with parameters p, a and b, whose probability density function (pdf) is

$$
f(x) \propto x^{p-1}\exp\left(-\frac{1}{2}\left(ax + \frac{b}{x}\right)\right). \tag{15}
$$

Note that we have the equivalence

$$\tau_{i,k}^2|m_{i,k},a_1,z_{i,k}\sim\mathcal{GIG}\left(\tau_{i,k}^2\left|\frac{1}{2},w_{i,k}^2a_1^2,\frac{m_{i,k}^2}{c_{1,k}}\right.\right)\quad\Leftrightarrow\quad\left.\frac{1}{\tau_{i,k}^2}\right|m_{i,k},a_1,z_{i,k}\sim\mathcal{IN}\left(\frac{1}{\tau_{i,k}^2}\left|\sqrt{\frac{a_1^2w_{i,k}^2c_{1,k}}{m_{i,k}^2}},a_1^2w_{i,k}^2\right.\right)\tag{16}$$

where $\mathcal{IN}(.|\mu,\lambda)$ is the inverse Gaussian distribution with parameters μ et λ whose pdf is

$$f(x)\propto x^{-3/2}\exp\left(-\frac{\lambda(x-\mu)^2}{2\mu^2x}\right).\tag{17}$$

Similar computations lead to

$$f(\tau_{i,k}^2|m_{i,k},a_{2,k}^2,z_{i,k})=\begin{cases}\mathcal{E}\left(\tau_{i,k}^2\left|\frac{2}{w_{i,k}^2a_2^2}\right.\right) & \text{if } z_{i,k}=0\\ \mathcal{GIG}\left(\tau_{i,k}^2\left|\frac{1}{2},w_{i,k}^2a_2^2,\frac{m_{i,k}^2}{c_{2,k}}\right.\right) & \text{if } z_{i,k}=1\end{cases},\quad i=s_k+1,...,2s_k\tag{18}$$

3.2 Conditional distribution of $z_{i,k}$

We will rather consider the marginal distribution of $z_{i,k}$, where $m_{i,k}$ has been marginalized, resulting into a partially collapsed Gibbs sampler (PCGS) and leading to better convergence properties [3]. The conditional distribution of $(m_{i,k},z_{i,k})$ for $i=1,...,s_k$ is given by

$$f(m_{i,k},z_{i,k}|y_{i,k},\boldsymbol{x}_{1,k},\tau_{i,k}^2,p_{1,k})\propto f(y_{i,k}|\boldsymbol{x}_{1,k},m_{i,k})f(m_{i,k}|z_{i,k},\tau_{i,k}^2)f(z_{i,k}|p_{1,k})\tag{19}$$

hence

$$\begin{aligned}&f(m_{i,k},z_{i,k}|y_{i,k},\boldsymbol{x}_{1,k},\tau_{i,k}^2,c_{1,k},p_{1,k})\propto\\&\exp\left(-\frac{(y_{i,k}-\bar{\boldsymbol{h}}_{i,k}\boldsymbol{x}_{1,k}-m_{i,k})^2}{2c_{1,k}\mu_{i,k}}\right)\left[\delta(m_{i,k})(1-z_{i,k})+\frac{\exp\left(-\frac{m_{i,k}^2}{2c_{1,k}\tau_{i,k}^2}\right)}{\sqrt{2\pi c_{1,k}\tau_{i,k}^2}}z_{i,k}\right][(1-p_{1,k})\delta(z_{i,k})+p_{1,k}\delta(1-z_{i,k})]=\\&\exp\left(-\frac{(y_{i,k}-\bar{\boldsymbol{h}}_{i,k}\boldsymbol{x}_{1,k}-m_{i,k})^2}{2c_{1,k}\mu_{i,k}}\right)\left[(1-p_{1,k})\delta(z_{i,k})\delta(m_{i,k})+p_{1,k}\delta(1-z_{i,k})\frac{\exp\left(-\frac{m_{i,k}^2}{2c_{1,k}\tau_{i,k}^2}\right)}{\sqrt{2\pi c_{1,k}\tau_{i,k}^2}}\right]=\\&\exp\left(-\tfrac{(y_{i,k}-\bar{\boldsymbol{h}}_{i,k}\boldsymbol{x}_{1,k})^2}{2c_{1,k}\mu_{i,k}}\right)(1-p_{1,k})\delta(z_{i,k})\delta(m_{i,k})+\exp\left(-\tfrac{(y_{i,k}-\bar{\boldsymbol{h}}_{i,k}\boldsymbol{x}_{1,k}-m_{i,k})^2}{2c_{1,k}\mu_{i,k}}\right)p_{1,k}\delta(1-z_{i,k})\tfrac{\exp\left(-\frac{m_{i,k}^2}{2c_{1,k}\tau_{i,k}^2}\right)}{\sqrt{2\pi c_{1,k}\tau_{i,k}^2}}.\end{aligned}\tag{20}$$

The marginal distribution of $z_{i,k}$ can then be computed as

$$\begin{aligned}f(z_{i,k}|y_{i,k},\boldsymbol{x}_{1,k},\tau_{i,k}^2,p_{1,k})&=\int_{\mathbb{R}}f(m_{i,k},z_{i,k}|y_{i,k},\boldsymbol{x}_{1,k},\tau_{i,k}^2,c_{1,k},p_{1,k})dm_{i,k}\\&\propto u_{i,k}\delta(z_{i,k})+v_{i,k}\delta(1-z_{i,k})\end{aligned}\tag{21}$$

with

$$\begin{aligned}u_{i,k}&=\int_{\mathbb{R}}\exp\left(-\frac{(y_{i,k}-\bar{\boldsymbol{h}}_{i,k}\boldsymbol{x}_{1,k})^2}{2c_{1,k}\mu_{i,k}}\right)(1-p_{1,k})\delta(m_{i,k})dm_{i,k}\\&=\exp\left(-\frac{(y_{i,k}-\bar{\boldsymbol{h}}_{i,k}\boldsymbol{x}_{1,k})^2}{2c_{1,k}\mu_{i,k}}\right)(1-p_{1,k})\end{aligned}\tag{22}$$

and

$$
\begin{aligned}
v_{i,k} =& p_{1,k} \int_{\mathbb{R}} \exp\left(-\frac{(y_{i,k} - \bar{\boldsymbol{h}}_{i,k}\boldsymbol{x}_{1,k} - m_{i,k})^2}{2c_{1,k}\mu_{i,k}}\right) \frac{\exp\left(-\frac{m_{i,k}^2}{2c_{1,k}\tau_{i,k}^2}\right)}{\sqrt{2\pi c_{1,k}\tau_{i,k}^2}} dm_{i,k} \\
=& \frac{p_{1,k}}{\sqrt{2\pi c_{1,k}\tau_{i,k}^2}} \int_{\mathbb{R}} \exp\left(-\frac{1}{2c_{1,k}}\left(\frac{(y_{i,k} - \bar{\boldsymbol{h}}_{i,k}\boldsymbol{x}_{1,k} - m_{i,k})^2}{\mu_{i,k}} + \frac{m_{i,k}^2}{\tau_{i,k}^2}\right)\right) dm_{i,k} \\
=& \frac{p_{1,k}}{\sqrt{2\pi c_{1,k}\tau_{i,k}^2}} \int_{\mathbb{R}} \exp\left(-\frac{1}{2c_{1,k}}\left(\frac{(y_{i,k} - \bar{\boldsymbol{h}}_{i,k}\boldsymbol{x}_{1,k})^2 - 2m_{i,k}(y_{i,k} - \bar{\boldsymbol{h}}_{i,k}\boldsymbol{x}_{1,k})}{\mu_{i,k}} + \left(\frac{1}{\mu_{i,k}} + \frac{1}{\tau_{i,k}^2}\right) m_{i,k}^2\right)\right) dm_{i,k} \\
=& \frac{p_{1,k}}{\sqrt{2\pi c_{1,k}\tau_{i,k}^2}} \\
& \times \int_{\mathbb{R}} \exp\left(-\frac{1}{2c_{1,k}\left(\frac{1}{\mu_{i,k}} + \frac{1}{\tau_{i,k}^2}\right)^{-1}}\left(\left(\frac{1}{\mu_{i,k}} + \frac{1}{\tau_{i,k}^2}\right)^{-1} \frac{(y_{i,k} - \bar{\boldsymbol{h}}_{i,k}\boldsymbol{x}_{1,k})^2 - 2m_{i,k}(y_{i,k} - \bar{\boldsymbol{h}}_{i,k}\boldsymbol{x}_{1,k})}{\mu_{i,k}} + m_{i,k}^2\right)\right) dm_{i,k}
\end{aligned}
\tag{23}
$$

Using the notations

$$
\begin{aligned}
\sigma_{m_{i,k}}^2 &= \left(\frac{1}{c_{1,k}\tau_{i,k}^2} + \frac{1}{c_{1,k}\mu_{i,k}}\right)^{-1} \\
&= \frac{c_{1,k}\mu_{i,k}\tau_{i,k}^2}{\mu_{i,k} + \tau_{i,k}^2}
\end{aligned}
\tag{24}
$$

$$
\begin{aligned}
\mu_{m_{i,k}} &= \sigma_{m_{i,k}}^2 \frac{(y_{i,k} - \bar{\boldsymbol{h}}_{i,k}\boldsymbol{x}_{1,k})}{c_{1,k}\mu_{i,k}} \\
&= \frac{\tau_{i,k}^2}{\mu_{i,k} + \tau_{i,k}^2}(y_{i,k} - \bar{\boldsymbol{h}}_{i,k}\boldsymbol{x}_{1,k}).
\end{aligned}
\tag{25}
$$

leads to

$$
\begin{aligned}
v_{i,k} &= \frac{p_{1,k}}{\sqrt{2\pi c_{1,k}\tau_{i,k}^2}} \int_{\mathbb{R}} \exp\left(-\frac{1}{2\sigma_{m_{i,k}}^2}\left(\sigma_{m_{i,k}}^2 \frac{(y_{i,k} - \bar{\boldsymbol{h}}_{i,k}\boldsymbol{x}_{1,k})^2 - 2m_{i,k}(y_{i,k} - \bar{\boldsymbol{h}}_{i,k}\boldsymbol{x}_{1,k})}{c_{1,k}\mu_{i,k}} + m_{i,k}^2\right)\right) dm_{i,k} \\
&= \frac{p_{1,k}}{\sqrt{2\pi c_{1,k}\tau_{i,k}^2}} \int_{\mathbb{R}} \exp\left(-\frac{1}{2\sigma_{m_{i,k}}^2}\left(\mu_{m_{i,k}}^2 \frac{c_{1,k}\mu_{i,k}}{\sigma_{m_{i,k}}^2} - 2m_{i,k}\mu_{m_{i,k}} + m_{i,k}^2\right)\right) dm_{i,k} \\
&= \frac{p_{1,k}}{\sqrt{2\pi c_{1,k}\tau_{i,k}^2}} \exp\left(-\frac{\mu_{m_{i,k}}^2 c_{1,k}\mu_{i,k}}{2(\sigma_{m_{i,k}}^2)^2}\right) \int_{\mathbb{R}} \exp\left(-\frac{1}{2\sigma_{m_{i,k}}^2}\left(-2m_{i,k}\mu_{m_{i,k}} + m_{i,k}^2\right)\right) dm_{i,k} \\
&= \frac{p_{1,k}}{\sqrt{2\pi c_{1,k}\tau_{i,k}^2}} \exp\left(-\frac{\mu_{m_{i,k}}^2 c_{1,k}\mu_{i,k}}{2(\sigma_{m_{i,k}}^2)^2}\right) \exp\left(\frac{\mu_{m_{i,k}}^2}{2\sigma_{m_{i,k}}^2}\right) \int_{\mathbb{R}} \exp\left(-\frac{\left(\mu_{m_{i,k}}^2 - 2m_{i,k}\mu_{m_{i,k}} + m_{i,k}^2\right)}{2\sigma_{m_{i,k}}^2}\right) dm_{i,k} \\
&= \frac{p_{1,k}}{\sqrt{2\pi c_{1,k}\tau_{i,k}^2}} \exp\left(-\frac{\mu_{m_{i,k}}^2 c_{1,k}\mu_{i,k}}{2(\sigma_{m_{i,k}}^2)^2}\right) \exp\left(\frac{\mu_{m_{i,k}}^2}{2\sigma_{m_{i,k}}^2}\right) \sqrt{2\pi\sigma_{m_{i,k}}^2}.
\end{aligned}
\tag{26}
$$

Moreover, using the equality

$$
\exp\left(-\frac{\mu_{m_{i,k}}^2 c_{1,k}\mu_{i,k}}{2(\sigma_{m_{i,k}}^2)^2}\right) = \exp\left(-\frac{(y_{i,k} - \bar{\boldsymbol{h}}_{i,k}\boldsymbol{x}_{1,k})^2}{2\mu_{i,k}c_{1,k}}\right)
\tag{27}
$$

we obtain

$$v_{i,k} = p_{1,k}\sqrt{\frac{\sigma^2_{m_{i,k}}}{c_{1,k}\tau^2_{i,k}}}\exp\left(-\frac{(y_{i,k}-\bar{\boldsymbol{h}}_{i,k}\boldsymbol{x}_{1,k})^2}{2\mu_{i,k}c_{1,k}}\right)\exp\left(\frac{\mu^2_{m_{i,k}}}{2\sigma^2_{m_{i,k}}}\right) \tag{28}$$

and the following Bernoulli distribution

$$f(z_{i,k}|y_{i,k},\boldsymbol{x}_{1,k},\tau^2_{i,k},p_{1,k}) = \mathcal{B}\left(z_{i,k}\left|\frac{v_{i,k}}{u_{i,k}+v_{i,k}}\right.\right), \quad i=1,...,s_k. \tag{29}$$

Note that $u_{i,k}$ and $v_{i,k}$ can be simplified to (as we only care about their ratio)

$$u_{i,k} = (1-p_{1,k}) \tag{30}$$

$$v_{i,k} = p_{1,k}\sqrt{\frac{\sigma^2_{m_{i,k}}}{c_{1,k}\tau^2_{i,k}}}\exp\left(\frac{\mu^2_{m_{i,k}}}{2\sigma^2_{m_{i,k}}}\right). \tag{31}$$

Similar computations lead to

$$f(z_{i,k}|y_{i,k},\boldsymbol{x}_{2,k},\tau^2_{i,k},p_{2,k}) = \mathcal{B}\left(z_{i,k}\left|\frac{v_{i,k}}{u_{i,k}+v_{i,k}}\right.\right), \quad i=s_k+1,...,2s_k \tag{32}$$

extending the definitions of $u_{i,k}$ and $v_{i,k}$ for $i=s_k+1,...,2s_k$ by

$$u_{i,k} = (1-p_{2,k}) \tag{33}$$

$$v_{i,k} = p_{2,k}\sqrt{\frac{\sigma^2_{m_{i,k}}}{c_{2,k}\tau^2_{i,k}}}\exp\left(\frac{\mu^2_{m_{i,k}}}{2\sigma^2_{m_{i,k}}}\right). \tag{34}$$

3.2.1 Conditional distribution of $m_{i,k}$

Going back to (20), we can also find the marginal distribution of $m_{i,k}$, for $i=1,...,s_k$, using the same computations and notations as before, yielding

$$f(m_{i,k}|y_{i,k},\boldsymbol{x}_{1,k},\tau^2_{i,k},z_{i,k}) \propto f(y_{i,k}|\boldsymbol{x}_{1,k},m_{i,k})f(m_{i,k}|z_{i,k},\tau^2_{i,k}) \tag{35}$$

i.e.,

$$f(m_{i,k}|y_{i,k},\boldsymbol{x}_{1,k},\tau^2_{i,k},z_{i,k}) = \begin{cases}\delta(m_{i,k}) & \text{if } z_{i,k}=0\\ \mathcal{N}(\mu_{m_{i,k}},\sigma^2_{m_{i,k}}) & \text{if } z_{i,k}=1\end{cases}, \quad i=1,...,s_k. \tag{36}$$

Similar computations lead to

$$f(m_{i,k}|y_{i,k},\boldsymbol{x}_{2,k},\tau^2_{i,k},z_{i,k}) = \begin{cases}\delta(m_{i,k}) & \text{if } z_{i,k}=0\\ \mathcal{N}(\mu_{m_{i,k}},\sigma^2_{m_{i,k}}) & \text{if } z_{i,k}=1\end{cases}, \quad i=s_k+1,...,2s_k \tag{37}$$

extending the definitions of $\mu_{m_{i,k}}$ and $\sigma^2_{m_{i,k}}$ for $i=s_k+1,...,2s_k$ with

$$\mu_{m_{i,k}} = \frac{\tau^2_{i,k}}{\mu_{i,k}+\tau^2_{i,k}}(y_{i,k}-\bar{\boldsymbol{h}}_{i,k}\boldsymbol{x}_{2,k}) \tag{38}$$

$$\sigma^2_{m_{i,k}} = \frac{c_{2,k}\mu_{i,k}\tau^2_{i,k}}{\mu_{i,k}+\tau^2_{i,k}}. \tag{39}$$

3.2.2 Conditional distribution of $\boldsymbol{x}_k$

We have

$$\begin{aligned}
f(\boldsymbol{x}_k|\boldsymbol{y}_k,\boldsymbol{m}_k) \propto & f(\boldsymbol{y}_k|\boldsymbol{x}_k,\boldsymbol{m}_k)f(\boldsymbol{x}_k) \\
& \propto \exp\left(-\frac{1}{2}(\boldsymbol{y}_k-\bar{\boldsymbol{H}}_k\boldsymbol{x}_k-\boldsymbol{m}_k)^T\boldsymbol{R}_k^{-1}(\boldsymbol{y}_k-\bar{\boldsymbol{H}}_k\boldsymbol{x}_k-\boldsymbol{m}_k)\right)\exp\left(-\frac{1}{2}\boldsymbol{x}_k^T(\boldsymbol{F}_k\boldsymbol{P}_{k|k}\boldsymbol{F}_k^T+\boldsymbol{Q}_k)^{-1}\boldsymbol{x}_k\right) \\
& \propto \exp\left(-\frac{1}{2}\left[\boldsymbol{x}_k^T\bar{\boldsymbol{H}}_k^T\boldsymbol{R}_k^{-1}(\boldsymbol{y}_k-\boldsymbol{m}_k)+\boldsymbol{x}_k^T(\bar{\boldsymbol{H}}_k^T\boldsymbol{R}_k^{-1}\bar{\boldsymbol{H}}_k+(\boldsymbol{F}_k\boldsymbol{P}_{k|k}\boldsymbol{F}_k^T+\boldsymbol{Q}_k)^{-1})\boldsymbol{x}_k\right]\right).
\end{aligned} \tag{40}$$

which is the following Gaussian distribution

$$f(\boldsymbol{x}_k|\boldsymbol{y}_k,\boldsymbol{m}_k) \sim \mathcal{N}(\boldsymbol{\mu}_{\boldsymbol{x}_k},\boldsymbol{\Sigma}_{\boldsymbol{x}_k}) \tag{41}$$

with

$$\boldsymbol{\Sigma}_{\boldsymbol{x}_k} = \left[\bar{\boldsymbol{H}}_k^T\boldsymbol{R}_k^{-1}\bar{\boldsymbol{H}}_k+(\boldsymbol{F}_k\boldsymbol{P}_{k|k}\boldsymbol{F}_k^T+\boldsymbol{Q}_k)^{-1}\right]^{-1} \tag{42}$$

$$\boldsymbol{\mu}_{\boldsymbol{x}_k} = \boldsymbol{\Sigma}_{\boldsymbol{x}_k}\bar{\boldsymbol{H}}_k^T\boldsymbol{R}_k^{-1}(\boldsymbol{y}_k-\boldsymbol{m}_k). \tag{43}$$

3.2.3 Conditional distribution of $a_{j,k}^2$

We have

$$\begin{aligned}
f(a_{1,k}^2|\boldsymbol{\tau}_k^2) &\propto f(\boldsymbol{\tau}_k^2|a_{1,k}^2)f(a_{1,k}^2) \\
&\propto \left(\prod_{i=1}^{s_k} f(\tau_{i,k}^2|a_{1,k}^2)\right) f(a_{1,k}^2) \\
&\propto \prod_{i=1}^{s_k} a_{1,k}^2 \exp\left(-\frac{w_{i,k}^2 a_{1,k}^2 \tau_{i,k}^2}{2}\right)(a_{1,k}^2)^{-1} \\
&\propto (a_{1,k}^2)^{s_k-1}\exp\left(-a_{1,k}^2\left(\frac{1}{2}\sum_{i=1}^{s_k} w_{i,k}^2\tau_{i,k}^2\right)\right).
\end{aligned} \tag{44}$$

A similar computation leads to a similar expression for $a_{2,k}$, with index i varying between s_k+1 and $2s_k$. Thus, defining $I_1=\{1,\ldots,s_k\}$ and $I_2=\{s_k+1,\ldots,2s_k\}$ we have the general result

$$f(a_{j,k}^2|\boldsymbol{\tau}_k^2) = \mathcal{G}\left(a_{j,k}^2 \,\middle|\, s_k, \frac{1}{2}\sum_{i\in I_j} w_{i,k}^2\tau_{i,k}^2\right). \tag{45}$$

3.2.4 Conditional distribution of $p_{j,k}$

Denoting as $\|\boldsymbol{z}_k\|_{0,j}$ the ℓ_0 pseudo-norm of the vector containing the element $z_{i,k}, i\in I_j$, the following result can be obtained

$$\begin{aligned}
f(p_{j,k}|\boldsymbol{z}_k) &\propto \prod_{i\in I_j, z_{i,k}=0}(1-p_{j,k})\prod_{i\in I_j, z_{i,k}=1} p_{j,k} \\
&\propto (1-p_{j,k})^{s_k-\|\boldsymbol{z}\|_{0,j}}p_{j,k}^{\|\boldsymbol{z}\|_{0,j}}
\end{aligned} \tag{46}$$

and thus

$$f(p_{j,k}|\boldsymbol{z}_k) = \mathcal{B}e\left(p_{j,k}\,|\|\boldsymbol{z}\|_{0,j}+1, s_k-\|\boldsymbol{z}\|_{0,j}+1\right). \tag{47}$$

4 Partially Collapsed Gibs Sampler (PCGS)

The proposed PCGS is given in Algorithm 1, whose purpose is to draw samples from the posterior distribution $f(\boldsymbol{x}_k, \boldsymbol{m}_k, \boldsymbol{z}_k, \boldsymbol{\tau}_k^2, \boldsymbol{a}_k, \boldsymbol{p}_k | \boldsymbol{y}_k)$. Once we have drawn enough realizations (n_{Gibbs}) and ensured that Markov chain has converged (after discarding the firsts $n_{\text{burn-in}}$ iterations belonging to the so-called the burn-in period), we can build the following estimators

$$\hat{\boldsymbol{z}} = \underset{\boldsymbol{z} \in \{0,1\}^{2s_k}}{\arg\max}\ \#\mathcal{M}(\boldsymbol{z}) \tag{48}$$

$$\hat{\boldsymbol{p}} = \frac{1}{\#\mathcal{M}(\hat{\boldsymbol{z}})} \sum_{m \in \mathcal{M}(\hat{\boldsymbol{z}})} \boldsymbol{p}^{(m)} \quad \text{where} \quad \boldsymbol{p} \in \{\boldsymbol{x}_k, \boldsymbol{m}_k, \boldsymbol{\tau}_k^2, \boldsymbol{a}_k, \boldsymbol{p}_k\} \tag{49}$$

where $\#A$ denotes the cardinal of the set A, $[\![a, b]\!]$ denotes the set of integers in $[a, b]$ and

$$\mathcal{M}(\boldsymbol{z}) = \{m \in [\![n_{\text{burn-in}} + 1, n_{\text{Gibbs}}]\!], \boldsymbol{z}^{(m)} = \boldsymbol{z}\}. \tag{50}$$

In other words, the indicator vector $\boldsymbol{z}$ is estimated by its MAP estimator and the other parameters by their MMSE estimators conditionally upon the estimated values of $\hat{\boldsymbol{z}}$.

Algorithme 1 Proposed PCGS

Initialization: $\boldsymbol{x}_k^{(0)}, \boldsymbol{m}_k^{(0)}, \boldsymbol{z}_k^{(0)}$ can be set tp their least squares estimators
Initialization: $a_{1,k}^{2(0)}, a_{2,k}^{2(0)}$ are set to 1 for instance
for $t = 1, ..., n_{\text{Gibbs}}$ **do**
  for $j = 1, 2$ **do**
    Draw $p_{j,k}^{(t)}$ according to $f(p_{j,k} | \boldsymbol{z}_k^{(t-1)})$
  end for
  for $i = 1$ to $2s_k$ **do**
    if $i \in \{1, \ldots, s_k\}$ **then**
      $j = 1$
    else if $i \in \{s_k + 1, \ldots, 2s_k\}$ **then**
      $j = 2$
    end if
    Draw $\tau_{i,k}^{2(t)}$ according to $f(\tau_{i,k}^2 | m_{i,k}^{(t-1)}, a_{j,k}^{2(t-1)}, z_{i,k}^{(t-1)})$
    Draw $z_{i,k}^{(t)}$ according to $f(z_{i,k} | y_{i,k}, \boldsymbol{x}_{j,k}^{(t-1)}, \tau_{i,k}^{2(t)}, p_{j,k}^{(t)})$
    Draw $m_{i,k}^{(t)}$ according to $f(m_{i,k} | y_{i,k}, \boldsymbol{x}_{j,k}^{(t-1)}, \tau_{i,k}^{2(t)}, z_{i,k}^{(t)})$
  end for
  for $j = 1, 2$ **do**
    Draw $a_{j,k}^{2(t)}$ according to $f(a_{j,k}^2 | \boldsymbol{\tau}_k^{2(t)})$
  end for
  Draw $\boldsymbol{x}_k^{(t)}$ according to $f(\boldsymbol{x}_k | \boldsymbol{y}_k, \boldsymbol{m}_k^{(t)})$
end for

Example of distributions obtained using the generated samples of $\boldsymbol{m}_k$ (upon the estimated values of $\hat{\boldsymbol{z}}_k$) are shown in figure 1. As one can see, we only estimate non-zero values. More specifically, we estimate satisfactory bias amplitudes for the nonzero values of the ground truth (non centered distributions) and small biases for the zero values of the ground truth (centered distributions). These estimates result in small bias estimates. However, non zero biases are obtained in each channel. To improve the detection results, we can use a Metropolis Hastings (MH) move proposing other values of $\boldsymbol{z}_k$ according to the value of $\mu_{m_{i,k}}$. More precisely, we can test if replacing a non-zero component of $\boldsymbol{z}_k$ with small amplitude can be set to zero, after accepting this move with the classical MH acceptance ratio.

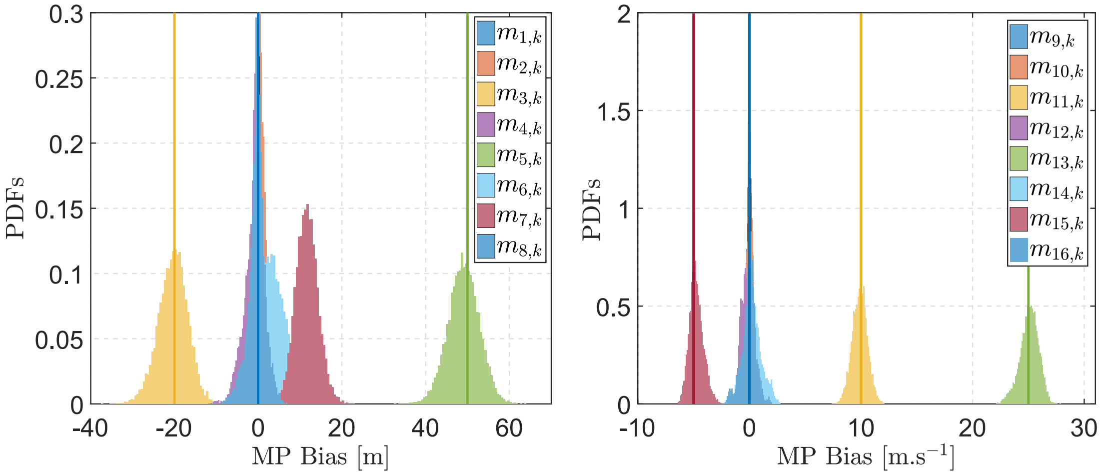

Figure 1: Estimated posteriors and ground truth (vertical lines) for MP biases affecting pseudoranges (left) and pseudorange rates (right) at fixed time instant. Note that three channels only (channels $\#3, 5$ and 7) are affected by MP biases.

5 Metropolis Hastings move

Despite its asymptotic convergence properties, the Gibbs sampler can be stuck around local minima [4, 5]. In this situation, its convergence can be accelerated by using appropriate Metropolis-Hastings (MH) moves. More precisely, using the ideas developed in [4] and [5], we have included MH moves, moving the indicators $\boldsymbol{z}$ in their neighborhood and accepting/rejecting these moves using the MH acceptance ratio. The idea is for instance to test whether a bias with low mean value $\mu_{m_{i,k}}$ can be set to 0 or not. To do so, we propose a new value of $\boldsymbol{z}$ denoted as $\bar{\boldsymbol{z}}$, generate the corresponding values of $\bar{\boldsymbol{m}}$ and $\bar{\boldsymbol{\tau}}$, and decide $\{\boldsymbol{z}, \boldsymbol{\tau}\} = \{\bar{\boldsymbol{z}}, \bar{\boldsymbol{\tau}}\}$ with the standard MH acceptance probability [6]. The proposed move is summarized in Algorithm 2 and was implemented with $\{\gamma_1, \eta_1, \gamma_2, \eta_2\} = \{1, 10, 1, 1\}$. This move is used in the PCGS before drawing $\boldsymbol{x}_k^{(t)}$ (hence the superscript $(t-1)$). The corresponding acceptance probability of this MH move can be computed as (using the independence between the different measurements)

$$f(\boldsymbol{z}_k, \boldsymbol{\tau}_k^2 | \boldsymbol{y}_k, \boldsymbol{x}_k, \boldsymbol{c}_k, \boldsymbol{p}_k, a_k) = \prod_{i=1}^{2s_k} f(z_{i,k}\tau_{i,k}^2 | y_{i,k}, \boldsymbol{x}_k, \boldsymbol{p}_k, \boldsymbol{a}_k^2) \tag{51}$$

and for $i \in \{1, ..., s_k\}$

$$
\begin{aligned}
f(z_{i,k}, \tau^2_{i,k}|.) &= \int_{\mathbb{R}} f(z_{i,k}, \tau^2_{i,k}, m_{i,k}|y_{i,k}, \boldsymbol{x}_{1,k}, p_{1,k}, a_{1,k})dm_{i,k} \\
&\propto \int_{\mathbb{R}} f(y_{i,k}|m_{i,k}, \boldsymbol{x}_{1k})f(m_{i,k}|z_{i,k}, \tau^2_{i,k})f(z_{i,k}|p_{1,k})f(\tau^2_{i,k}|a^2_{1,k})dm_{i,k} \\
&\propto \int_{\mathbb{R}} \exp\left(-\frac{(y_{i,k}\bar{\boldsymbol{h}}_{i,k}\boldsymbol{x}_{1,k} - m_{i,k})^2}{2c_{1,k}\mu_{i,k}}\right)\left[\delta(m_{i,k})(1 - z_{i,k}) + \frac{\exp\left(-\frac{m^2_{i,k}}{2c_{1,k}\tau^2_{i,k}}\right)}{\sqrt{2\pi c_{1,k}\tau^2_{i,k}}} z_{i,k}\right] \\
&\quad \times [(1 - p_{1,k})\delta(z_{i,k}) + p_{1,k}\delta(1 - z_{i,k})] \exp\left(-\frac{w^2_{i,k}a^2_{1,k}\tau^2_{i,k}}{2}\right)dm^2_{i,k} \\
&\propto \int_{\mathbb{R}} \exp\left(-\frac{(y_{i,k}\bar{\boldsymbol{h}}_{i,k}\boldsymbol{x}_{1,k} - m_{i,k})^2}{2c_{1,k}\mu_{i,k}}\right)\left[(1 - p_{1,k})\delta(z_{i,k})\delta(m_{i,k}) + p_{1,k}\frac{\exp\left(-\frac{m^2_{i,k}}{2c_1\tau^2_{i,k}}\right)}{\sqrt{2\pi c_{1,k}\tau^2_{i,k}}}\delta(1 - z_{i,k})\right] dm_{i,k} \qquad (52) \\
&\quad \times \exp\left(-\frac{w^2_{i,k}a^2_{1,k}\tau^2_{i,k}}{2}\right) \\
&\propto \left[\frac{u_{i,k}}{u_{i,k} + v_{i,k}}\delta(z_{i,k}) + \frac{v_{i,k}}{u_{i,k} + v_{i,k}}\delta(1 - z_{i,k})\right] \exp\left(-\frac{w^2_i a^2_1 \tau^2_{i,k}}{2}\right) \qquad (53)
\end{aligned}
$$

with $u_{i,k}$, $v_{i,k}$ as defined in (33) and (34). Note that we had to make sure that the term between brackets sums to 1 (i.e., divide by $u_{i,k} + v_{i,k}$), because the terms $u_{i,k}$ and $v_{i,k}$ both depend on $\tau^2_{i,k}$. Then,

$$
f(z_{i,k}, \tau^2_{i,k}|y_{i,k}, \boldsymbol{x}_1, p_{1,k}, a^2_{1,k}) \propto \begin{cases} \frac{1-p_{1,k}}{1-p_{1,k}+p_{1,k}\sqrt{\frac{\sigma^2_{m_{i,k}}}{c_{1,k}\tau^2_{i,k}}}\exp\left(\frac{\mu^2_{m_{i,k}}}{2\sigma^2_{m_{i,k}}}\right)} \exp\left(-\frac{w^2_i a^2_1 \tau^2_{i,k}}{2}\right) & \text{if } z_{i,k} = 0 \\ \frac{p_{1,k}\sqrt{\frac{\sigma^2_{m_{i,k}}}{c_{1,k}\tau^2_{i,k}}}\exp\left(\frac{\mu^2_{m_{i,k}}}{2\sigma^2_{m_{i,k}}}\right)}{1-p_{1,k}+p_{1,k}\sqrt{\frac{\sigma^2_{m_{i,k}}}{c_1\tau^2_{i,k}}}\exp\left(\frac{\mu^2_{m_{i,k}}}{2\sigma^2_{m_{i,k}}}\right)} \exp\left(-\frac{w^2_i a^2_1 \tau^2_{i,k}}{2}\right) & \text{if } z_{i,k} = 1 \end{cases}, i = 1, ..., s_k. \qquad (54)
$$

Similar computations lead to

$$
f(z_{i,k}, \tau^2_{i,k}|y_{i,k}, \boldsymbol{x}_2, p_{2,k}, a^2_{2,k}) \propto \begin{cases} \frac{1-p_{2,k}}{1-p_{2,k}+p_{2,k}\sqrt{\frac{\sigma^2_{m_{i,k}}}{c_{2,k}\tau^2_{i,k}}}\exp\left(\frac{\mu^2_{m_{i,k}}}{2\sigma^2_{m_{i,k}}}\right)} \exp\left(-\frac{w^2_i a^2_2 \tau^2_{i,k}}{2}\right) & \text{if } z_{i,k} = 0 \\ \frac{p_{2,k}\sqrt{\frac{\sigma^2_{m_{i,k}}}{c_{2,k}\tau^2_{i,k}}}\exp\left(\frac{\mu^2_{m_{i,k}}}{2\sigma^2_{m_{i,k}}}\right)}{1-p_{2,k}+p_{2,k}\sqrt{\frac{\sigma^2_{m_{i,k}}}{c_2\tau^2_{i,k}}}\exp\left(\frac{\mu^2_{m_{i,k}}}{2\sigma^2_{m_{i,k}}}\right)} \exp\left(-\frac{w^2_i a^2_2 \tau^2_{i,k}}{2}\right) & \text{if } z_{i,k} = 1 \end{cases}, i=s_k+1,...,2s_k.
$$

Example of posterior distributions from the paper [1] for $\boldsymbol{m}_k$ (given the estimated values of $\hat{\boldsymbol{z}}_k$) drawn from the proposed sampler including the MH move are displayed in Fig. 2. As one can see, the detection is much more efficient with this method, as we only estimate the bias amplitudes associated with the channels affected by multipath.

6 Simulation scenarios

The data were simulated using a real receiver trajectory (displayed in Fig. 3) and 8 real satellite positions from a measurement campaign. The 16 corresponding measurements (8 pseudoranges

Algorithme 2 Metropolis Hastings move

Initialization $\bar{\boldsymbol{z}}_k = \boldsymbol{z}_k^{(t)}$
for $i = 1$ to $2s_k$ **do**
  if $i \in \{1, \ldots, s_k\}$ **then**
    $j = 1$
  else if $i \in \{s_k + 1, \ldots, 2s_k\}$ **then**
    $j = 2$
  end if
  Set $\bar{z}_{i,k}$ corresponding to $|\mu_{m_{i,k}}| < \gamma_j$ to 0
  Set $\bar{z}_{i,k}$ corresponding to $|\mu_{m_{i,k}}| > \eta_j$ to 1
  Draw $\bar{m}_{i,k}$ from $f(\bar{m}_{i,k}|y_{i,k}, \boldsymbol{x}_{j,k}^{(t-1)}, \tau_{i,k}^{2(t)}, \bar{z}_{i,k})$
  Draw $\bar{\tau}_{i,k}^2$ from $f(\bar{\tau}_{i,k}^2|\bar{m}_{i,k}, a_{j,k}^2, \bar{z}_{i,k})$
end for
Set $\{\boldsymbol{z}_k^{(t)}, \boldsymbol{\tau}_k^{2(t)}\} = \{\bar{\boldsymbol{z}}_k, \bar{\boldsymbol{\tau}}_k^2\}$ with probability $\min\left(\frac{f(\bar{\boldsymbol{z}}_k, \bar{\boldsymbol{\tau}}_k^2|\boldsymbol{y}_k, \boldsymbol{x}_k, \boldsymbol{p}_k, \boldsymbol{a}_k)}{f(\boldsymbol{z}_k^{(t)}, \boldsymbol{\tau}_k^{2(t)}|\boldsymbol{y}_k, \boldsymbol{x}_k, \boldsymbol{p}_k, \boldsymbol{a}_k)}, 1\right)$
if Proposal is accepted **then**
  Draw $\boldsymbol{m}_k$ from $f(\boldsymbol{m}_k|\boldsymbol{y}_k, \boldsymbol{x}_{j,k}^{(t-1)}, \boldsymbol{\tau}_k^{2(t)}, \boldsymbol{z}_k^{(t)})$
end if

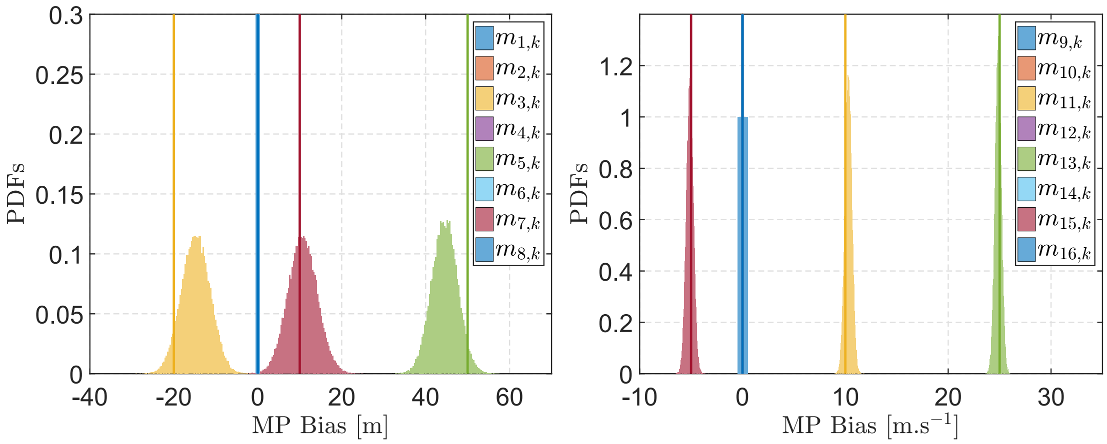

Figure 2: Estimated posteriors and ground truth (vertical lines) for MP biases affecting pseudoranges (left) and pseudorange rates (right) at fixed time instant. Note that three channels only (channels #3, 5 and 7) are affected by MP biases and that they are the only ones detected by the proposed method when using the MH move.

and 8 pseudorange rates) were generated according to Eq. (6) of the paper, where $\boldsymbol{x}_k$ was generated according to the reference trajectory, $\boldsymbol{n}_k$ according to (7). The values of C/N_0 and the vector $\boldsymbol{m}_k$ were generated according to Table 1. More precisely, for $k \notin \{50, ..., 130\}$, the value of C/N_0 for the different satellites were fixed to 45 dBHz, 43 dBHz, 45 dBHz, 42 dBHz, 43 dBHz, 45 dBHz, 43 dBHz and 45 dBHz. When $k \in \{50, ..., 130\}$, we changed the C/N_0 values of the third, fifth and seventh satellites to 35, 32 and 34 dBHz. The multipath bias vector $\boldsymbol{m}_k$ was fixed to zero for $k \notin \{50, ..., 130\}$. When $k \in \{50, ..., 130\}$ we added biases to satellites 3, 5 and 7, equal to -20, 50 and 10 meters for the pseudoranges, and 10, 25 and -5 meters per second for the pseudorange rates.

Parameter	Value
$C/N_{0,k}, k \notin \{50, ..., 130\}$	$(45, 43, 45, 42, 43, 45, 43, 45)$
$C/N_{0,k}, k \in \{50, ..., 130\}$	$(45, 43, 35, 42, 32, 45, 34, 45)$
$\boldsymbol{m}_{1:8,k}, k \notin \{50, ..., 130\}$	$(0, 0, 0, 0, 0, 0, 0, 0)$
$\boldsymbol{m}_{1:8,k}, k \in \{50, ..., 130\}$	$(0, 0, -20, 0, 50, 0, 10, 0)$
$\boldsymbol{m}_{9:16,k}, k \notin \{50, ..., 130\}$	$(0, 0, 0, 0, 0, 0, 0, 0)$
$\boldsymbol{m}_{9:16,k}, k \in \{50, ..., 130\}$	$(0, 0, 10, 0, 25, 0, -5, 0)$

Table 1: Simulation parameters.

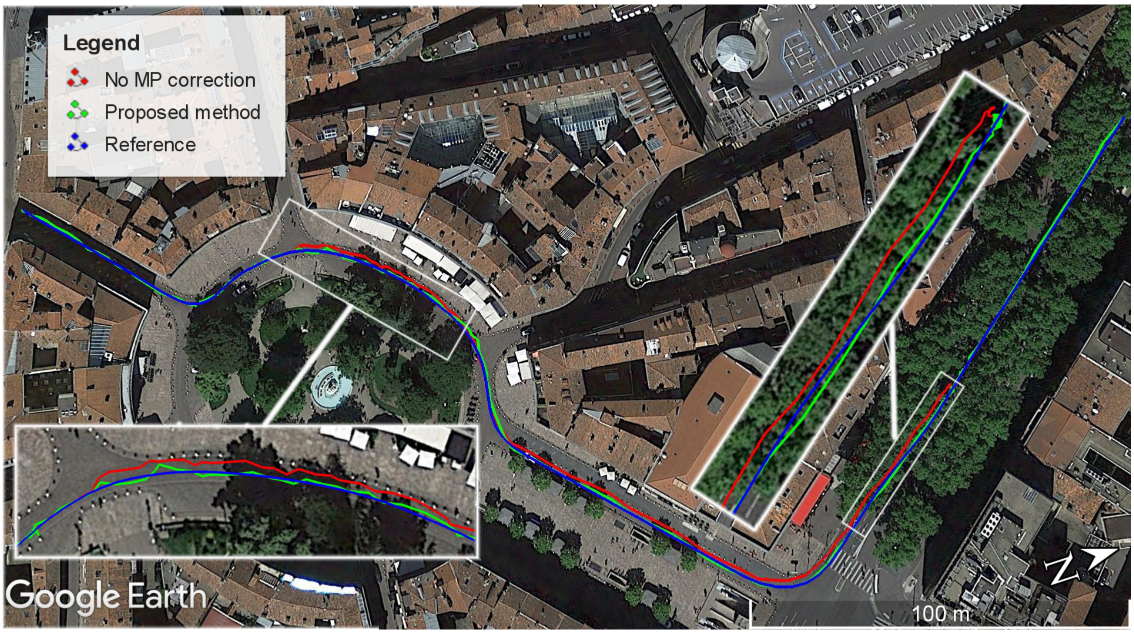

Figure 3: Reference and estimated trajectories (for one Monte-Carlo realization) with and without MP detection/correction.

7 Simulation results

Figure 4 and 5 show the mean estimated biases over 100 Monte-Carlo runs, the corresponding ground truth and the $\pm\sigma$ variation versus time on pseudoranges and pseudorange rates respectively. The corresponding position errors are given in figure 6.

We also challenged the proposed algorithm to more realistic scenarios including time-varying multipath biases. More precisely, the biases were generated according to the following dynamics $m_{i,t+1} = m_{i,t} + n_i$ where $n_i \sim \mathcal{N}(0, \sigma^2_{i,m})$ for $i = 1, ..., 2s_k$ and $\sigma^2_{i,m} = 0.1$m for the pseudoranges

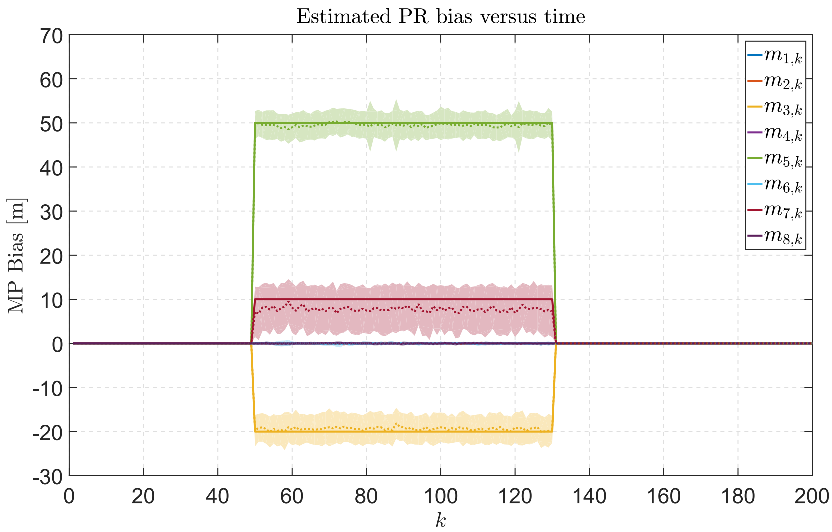

Figure 4: Ground truth (plain) and estimated biases (dotted) for with their $\pm\sigma$ variations pseudoranges versus time (100 Monte Carlo runs).

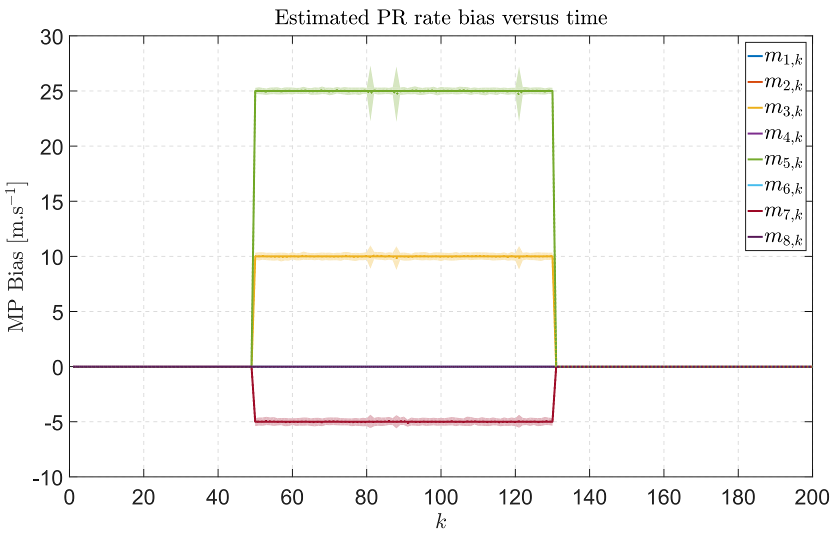

Figure 5: Ground truth (plain) and estimated biases (dotted) with their $\pm\sigma$ variations for pseudorange rates versus time (100 Monte Carlo runs).

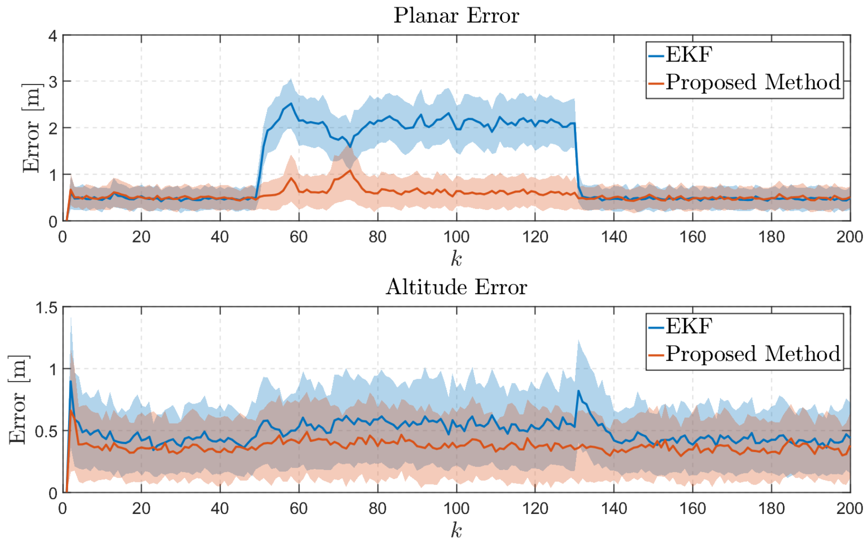

Figure 6: Planar and altitude errors for the EKF and the proposed method versus time (100 Monte Carlo runs) and their standard deviations.

$(i = 1, ..., s_k)$ and $\sigma^2_{i,m} = 0.01\text{m.s}^{-1}$ for the pseudorange rates $(i = s_k + 1, ..., 2s_k)$. The results are displayed in Fig. 7 for the pseudoranges and 8 for the pseudorange rates. The corresponding position errors are displayed in Fig. 9. As we can observe, the biases are well estimated, even if the amplitude estimates have more variance (especially for satellite #3 for instance, where we can notice a gap in the amplitude estimate although the corresponding measurement is detected as biased). Note that the improvement in positioning errors is also clear for this example.

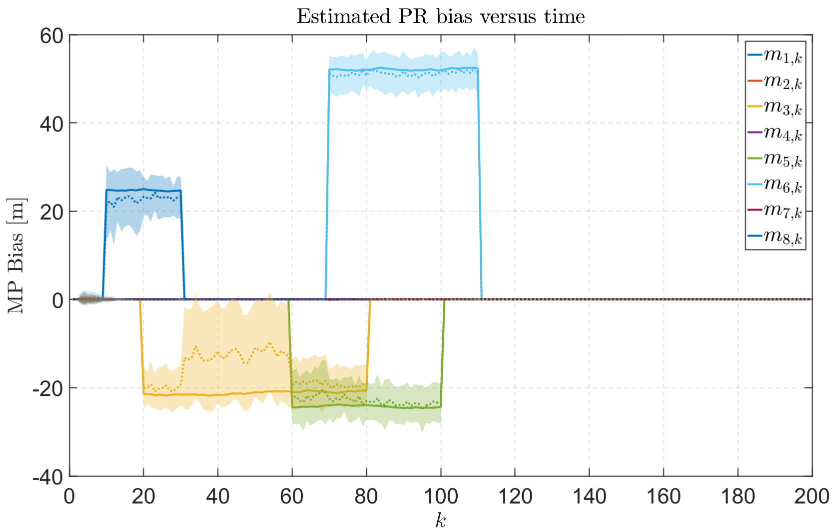

Figure 7: Ground truth (plain) and estimated biases (dotted) with their $\pm\sigma$ variations for pseudoranges versus time (100 Monte Carlo runs).

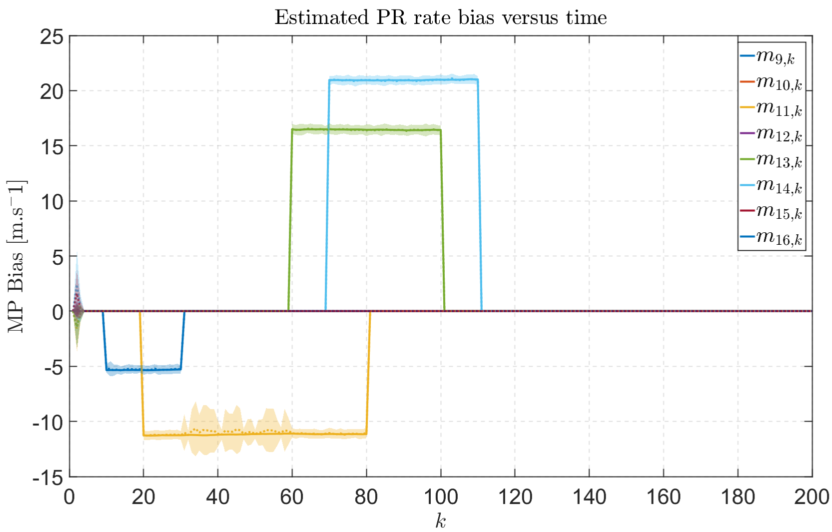

Figure 8: Ground truth (plain) and estimated biases (dotted) with their $\pm\sigma$ variations for pseudorange rates versus time (100 Monte Carlo runs).

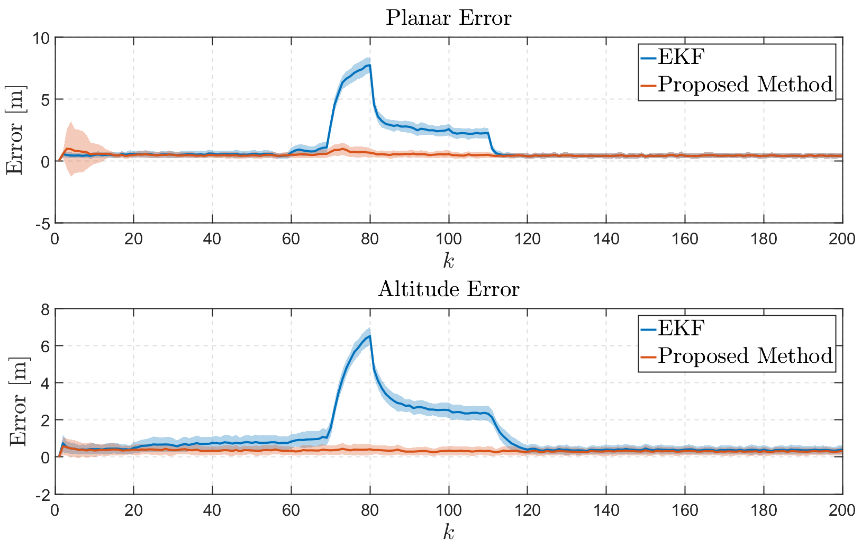

Figure 9: Planar and altitude errors for the EKF and the proposed method versus time (100 Monte Carlo runs) and their standard deviations.

References

[1] J. Lesouple, J.-Y. Tourneret, M. Sahmoudi, F. Barbiero, and F. Faurie, "Multipath Mitigation in Global Navigation Satellite Systems Using a Bayesian Hierarchical Model with Bernoulli Laplacian Priors," in *Proc. IEEE Workshop on Stat. Signal Processing (SSP)*, Freiburg, Germany, June 2018, pp. xx–xx.

[2] P. D. Groves and Z. Jiang, "Height Aiding, C/N_0 Weighting and Consistency Checking for GNSS NLOS and Multipath Mitigation in Urban Areas," *Journal of Navigation*, vol. 66, no. 5, pp. 653–669, 2013.

[3] D. A. Van Dyk and T. Park, "Partially Collapsed Gibbs Samplers: Theory and Methods," *Journal of the American Statistical Association*, vol. 103, no. 482, pp. 790–796, June 2008.

[4] S. Bourguignon and H. Carfantan, "Bernoulli-Gaussian Spectral Analysis of Unevenly Spaced Astrophysical Data," in *Proc. IEEE Workshop on Stat. Signal Processing (SSP)*, Bordeaux, France, July 2005, pp. 811–816.

[5] F. Costa, H. Batatia, T. Oberlin, C. D'Giano, and J.-Y. Tourneret, "Bayesian EEG Source Localization Using a Structured Sparsity Prior," *NeuroImage*, vol. 144, pp. 142 – 152, 2017.

[6] C. Robert and G. Casella, *Monte Carlo Statistical Methods.* Springer-Verlag New York, 2004.